## REFERENCES


1. Garg , D.R. , and D.M. Ruthven , " Performances of Molecular Sieve Adsorption Column : Combined Effects of Mass Transfer and Longitudinal Diffusion ", Chem. Engng. Sci., 30(9) , 1192-1194 , 1975 .

2. Ruthven , D.M., Principle of Adsorption and Adsorption Processes, pp.204-219 , John Wiley & sons Inc. , 1984 .

3. Bella , L.Z. , and T.W. Weber , " Axial Dispersion of Gases in Packed Beds " , AIChE J. , 15(1) , 146-149, 1969 .

4. Carberry , J.J. , and R.H. Bretton , " Axial Dispersion of Mass in Flow Through Fixed Beds ", AIChE J. , 4(3), 367-375 , 1958 .

5. Chao , R., and H.E.Hoelscher , " Simultanesous Axial Dispersion and Adsorption in a Packed Bed " , AIChE J. , 12(2) , 271-278 , 1966 .

6. Edwards , M.F. , and Richardson , J.F. , " Gas Dispersion in Packed Beds ", Chem. Engng. Sci., 23(1) , 109-114 ,1968 .

7. Evan , E.V. , and Kenney , C.N. , " The Dispersion of Gas in Flow Through a Bed of Packed Solid " , Trans. Inst. Chem. Engrs. , 44(1) , 189 -193 , 1966 .

8. Mc Henry , K.W. , JR. , and R.H. Wilhelm , " Axial Mixing of Binary Gas Mixtures Flowing in a Random Bed of Spheres " , AIChE J. , 3(1) , 83-91 , 1957 .

9. Volkov , S.A. , V.I. Reznikov , K.F. Khalilov , V.Yu. Zel'vensky, and K.I. Sakodynsky , " Nonuniformity of Packed Beds and Its Influence on Longitudinal Dispersion " , Chem. Engng. Sci. , 41(2) , 389-397 , 1986 .

10. Deans , H.A. , and L. Lapidus , " A Computational Model for Predicting and Correlating the Behavior of Fixed-Bed Reactors I : Derivation of Model for Non-Reactive Systems " , AIChE J. , 6(1) , 656 , 1960 .

11. Hinduja , M.J. , S. Sundaresan , and R. Jackson , " A Crossflow Model Of Dispersion in Packed Bed Reactors " , AIChE J. , 26(2) , 274-281 , 1980 .

12. Carbonell , R.G. , " Flow Nonuniformities in Packed Beds : Effect on dispersion ", Chem. Engng. Sci.,35(2), 1347-1351,1980.

13. Klingman , K.J. , and H.H. Lee , " alternating Flow Model for Mass and Heat Dispersionin Packed Beds " , AIChE J. , 33(3) , 366-381 , 1987 .

14. Kreft , A. , and A. Zuber , " On The Physical Meaning of the Dispersion Equation and Its Solutions for Different Initial and Boundary Conditions " , Chem. Engng. Sci. , 33(1) , 1471-1480 , 1978 .

15. Paralekar , S.J. , and D. Ramkrishna , " Analysis of Axially Dispersed Systems with General Boundary Conditions – I , Chem. Engng. Sci. , 39(11) , 1571-1579 , 1984 .

16. Paralekar , S.J. , and D. Ramkrishna , " Analysis of Axially Dispersed Systems with General Boundary Conditions – II , Chem. Engng. Sci. , 39(11) , 1581-1597 , 1984 .

17. Paralekar , S.J. , and D. Ramkrishna , " Analysis of Axially Dispersed Systems with General Boundary Conditions – III, Chem. Engng. Sci. , 39(11) , 1599-1611 , 1984 .

18. Kolev , S.D. , and E. Pungor ," Numerical Solution of Hydraulic Models Based on The Axially-dispersed Plug Flow Model by Laplace Transforms " , Analytica Chimica Acta , 194(1) , 61-75 , 1987 .

19. Langer G., Roethe A., K-P. Rothe , and D. Gelbin , " Longitudinal Mixing in Packed Bed " , Int. J. Heat and Mass Trans. , 21(1) ,751-760 , 1978 .

20. Gun , D.J. , " Axial and Radial Dispersion in Fixed Beds " , Chem. Engng. Sci. , 42(2) , 363-373 , 1987 .

21. Aris , R. , and Amundson , N.R. , " Flow Distribution in Packed Beds " ,AICHE J. , 3 , 280 (1957).

22. Wen , C.Y. , and L.T Fan , Model for Flow systems and Chemical Reactors , Marcel Dekker Inc. , New York , 1975 .

23. Carberry , J.J. , " Axial Dispersion and Void-cell Mixing Efficiency in Fluid Flow in Fixed Beds ", AICHE J., 4(1), 13M-20M , 1958 .

24. Lavenspiel , O. , Chemical Reaction Engineering , pp. 253 - 308 , John Wiley & Sons Inc. , 1972 .

25. Smith , J.M. , Chemical Engineering Kinetics , pp.243 - 263 , McGraw - Hill Book Company , 1970 .

26. Oliveros , G. , and J.M. Smith , " Dynamic Studies of Dispersion and Channeling in Fixed Beds " , AICHE J. , 28(5) , 1982 .

27. Wilhelm , A.M. , " Etude D'une Colonne De Chromatographie Liquide Liquide Preparative Analyse de L'ecoulement et des Transferts de Matiere , " Ph.D. thesis , L'institut National Polytechnique de Toulouse , 1983 .

28. Yano ,T, and Aratani, T., " Boundary Conditions of Flow Reactor " Seigyo Kogaku , 12 , 18 (1968) .

29. Stephanopoulos , G., Chemical Process Control An Introduction to Theory and Practice , Prentice Hall Inc. , New Jersey , 1984 .

30. Smith , J.M. , and C.E. Schwartz , " Flow Distribution in Packed Beds " , Ind. Eng. Chem. , 45(6) , 1209-1218 , 1953 .

31. Han , N.W. , J. Bhakta , and R.G. Carbonell , " Longitudinal and Lateral Dispersion in Packed Beds : Effect of Column Length and Particle Size Distribution " , AIChE J. , 31(2) , 277-280 , 1985 .

32. Hsiang , T.C. , and H.W. Haynes , " Axial dispersion in small Diameter Bed of Large Spherical Particles " , Chem. Engng. Sci. , 32(1) , 678-681 , 1977 .

33. Young , L.C , and B.A. Finlayson , " Axial Dispersion in Non-isothermal Packed Bed Chemical Reactors " , Ind. Engng. Chem. Fundl. , 12(4) , 412-422 , 1973 .

34.Scott , D.S., Lee W. , and Papa J., " The Measurement of Transport Coefficients in Gas-solid Heterogeneous Reactions " , Chem. Engng. Sci. , 29(11) , 2155-2167 , 1974 .

35 Taylor G. , " Dispersion in Packed Beds " , Proc. Royal Soc. , series A 219 , 186-192 , 1961 .

36. Reid , C.R , and T.K. Sherwood , The Properties of Gases and Liquids , McGraw Hill Book Company Inc. , New york , 1958 .

# APPENDIX

# APPENDIX A

## RELATIONSHIP BETWEEN AXIAL DISPERSION COEFFICIENT AND VELOCITY AND PARTICLE SIZE

Let us follow the viewpoint that packed beds consist of series of randomly arrayed void cells through which fluid flows with some mixing . So a mixing efficiency is a function of turbulence and retention time for a given fluid , it follows that fluid velocity and cell size controls mixing efficiency . Cell size is a function of particle diameter . Thus it may be written ( 25 ) as

$$E_z = k*d_p*u \quad \text{or} \quad d_p*u/E_z = 1/k = Pe \qquad \text{A.1}$$

For a given velocity , a mixing time , provided by the cell dimension and the number of such cells , is required for perfect mixing . However , the situation which is characterized by imperfect mixing will have a cell retention time $\theta_n$ less than that of a perfect cell $\theta_p$ . Therefore more than one cell is required to achieve the perfect mixing time . For a bed of $n_p$ void cells , the effect of imperfect mixing is to endow the bed with dispersion characteristics of a bed of n mixers . Since $n < n_p$ , a greater dispersion and thus larger E results .

Imperfect mixing may be viewed as the result of by-passing or short circuiting and dead-space retention . This states that a fraction of particles entering void cells passes through in a much shorter time than the holding time $\theta_n$ , while other fractions retained for much greater periods than this holding time . Obviously a distribution of retention times results is characterized by a dispersion coefficient E . The similarity of this process to molecular diffusion offers an opportunity for a more quantitative treatment .

Consider a field of particles and a zone $(x_2-x_1)$ bound by line $P_1$ and $P_2$ as shown in figure A1 .

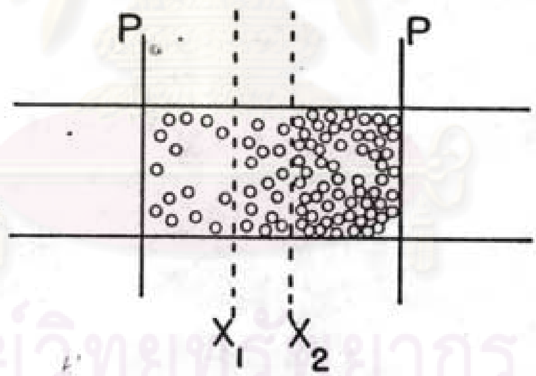


**Fig. Einstein's kinetic-diffusion model.**



Fig. A.1 Einstein's kinetic-diffusion model

The transport of U molecules from left to right per unit area can be expressed as

$$U_a = 1/2 * c_a * (x_2-x_1) \qquad \text{A.2}$$

Imperfect mixing may be viewed as the result of by-passing or short circuiting and dead-space retention . This states that a fraction of particles entering void cells passes through in a much shorter time than the holding time $\theta_n$ , while other fractions retained for much greater periods than this holding time . Obviously a distribution of retention times results is characterized by a dispersion coefficient E . The similarity of this process to molecular diffusion offers an opportunity for a more quantitative treatment .

Consider a field of particles and a zone $(x_2-x_1)$ bound by line $P_1$ and $P_2$ as shown in figure A1 .

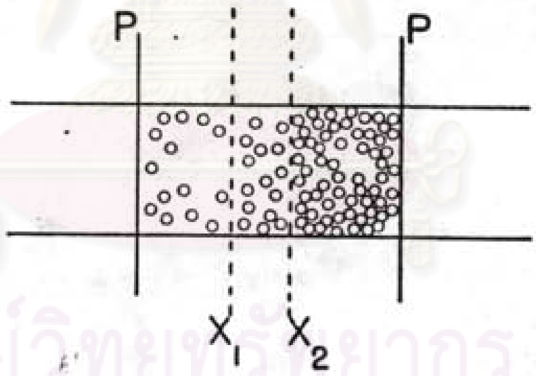


Fig. Einstein's kinetic-diffusion model.

Fig. A.1 Einstein's kinetic-diffusion model

The transport of U molecules from left to right per unit area can be expressed as

$$U_a = 1/2*c_a*(x_2-x_1) \qquad A.2$$

If a real packed bed of length L is visualized as n mixing units , then the height of one mixer is L/n . By measuring upstream and downstream dispersion or diffusion , the mixing coefficient E is obtained . Therefore the time constant for axial mixing can be expressed in a similar manner as equation A.6

$$\theta_a = (L/n)^2/2E \qquad \text{A.7}$$

As the holding time per mixing length for a bed velocity u is

$$\theta_n = \frac{L/n}{u}$$

since a perfect mixer is one in which retention time equals mixing time then

$$\frac{L/n}{u} = (L/n)^2/2E$$

or

$$n = Lu/2E \qquad \text{A.9}$$

To relate this expression with the ideal perfect mixer formed by particles of diameter $d_p$ , a mixing efficiency e is introduced here and defined as a ratio of actual mixers n to the limiting number in the ideal perfect mixer ($n_p$) ; $e = n/n_p$ . Since the length of each perfect mixing cell will be some fraction (F) of particle diameter $d_p$ , the constant fraction F will be about unity or less depending on the packing arrangements , therefore the number of perfect mixers is

$$n_p = L/(F*d_p) \qquad A.10$$

From equation A.9 and A.10 , mixing efficiency becomes

$$e = (Lu/2E)/(L/Fd_p) = (F/2)(d_pu/E)$$

or

$$e/F = 1/2*(d_pu/E) \qquad A.11$$

For diffusion behaviour in the void cell approaches the ideal perfect mixer , e-->1 and F is approximately 1 , thus e/F called mixing length for the bed becomes unity and equation A.11 can be expressed as

$$E = 1/2*d_p*u \qquad A.12$$

# APPENDIX B

## DERIVATION OF THE MODEL'S TRANSFER FUNCTION

Consider the following system

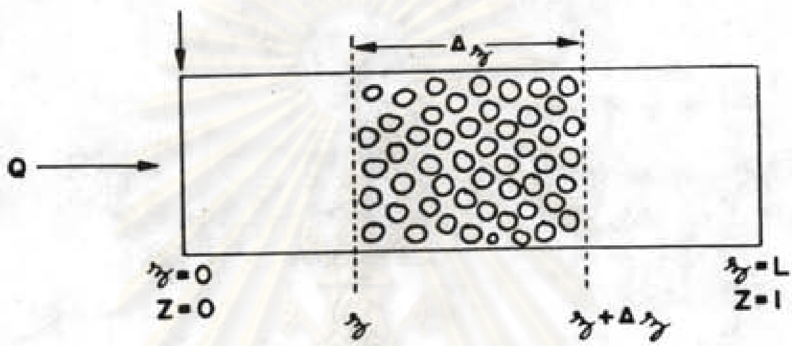


Fig. B1 Packed Bed System

Assumptions

1. No reactions occur
2. Fluid velocity remains constant
3. Radial velocity gradients do not exist

Then the material balance around this system is

$$\epsilon * A * \Delta z * \frac{\partial c(z,t)}{\partial t} = Q[c(z,t)-c(z+\Delta z,t] + E_z * A * \left[ \frac{\partial c(z+\Delta z,t)}{\partial z} - \frac{\partial c(z,t)}{\partial z} \right]$$

dividing the above equation by A*Δz   we obtain

$$\epsilon \frac{\partial c}{\partial t} = \frac{Q}{A} * \left[\frac{c(z,t)-c(z+ z,t)}{\Delta z}\right] + E_z\left[\frac{\partial(c(z+\Delta z,t/\partial z)-\partial c(z,t)/\partial z)}{\partial z}\right]$$

It ultimately yields

$$\partial c/\partial t \quad = \quad -u_z * \partial c/\partial z \quad + \quad E_z[\partial^2 c/\partial z^2] \qquad \text{B.1}$$

| Accumulation term | convection term | dispersion term |
|---|---|---|

Let $Z = z/L$ , $\tau = \epsilon * L/u_z$ , $Pe = L * u_z/E_z$

Therefore equation B.1 can be rewritten in dimensionless form as

$$1/Pe*(\partial^2 c/\partial Z^2) \quad - \quad \partial c/\partial Z \quad = \quad \tau * (\partial c/\partial t) \qquad \text{B.2}$$

Before applying a closed-closed boundary condition to equation B.2 , let us focus on mass conservation at the inlet point and the outlet point , respectively .



At inlet point

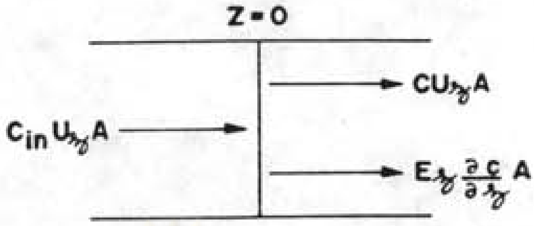


Fig.b2 Mass Conservation at The Inlet Point

$$A*u_z*c_{in}(z=0,t) = A*u_z*c(z=0,t) - A*E_z*[\partial c(z=0,t)/\partial z]$$

or

$$c_{in}(z=0,t) = c(z=0,t) - (E_z/u_z)*[\partial c(z=0,t)/\partial z]$$

now let $Z = z/L$ ,and $u_z*L/E_z = Pe$

so

$$c_{in}(z=0,t) = c(z=0,t) - (1/Pe)*[\partial c(z=0,t)/\partial z] \qquad B.3$$

At outlet point

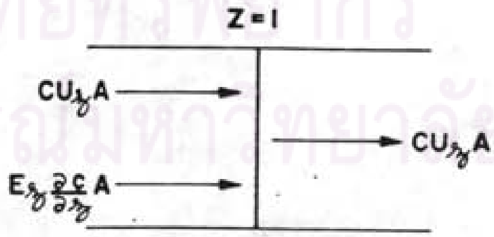


Fig.B3 Mass Conservation at The Outlet point

$$A*u_z*c_s(z=L,t) - A*E_z*[\partial c(z=L,t)/\partial z] = A*u_z*c_e(z=L,t)$$

or

$$c_s(z=L,t) - (E_z/u_z)*[\partial c(z=L,t)/\partial z] = c_e(z=L,t)$$

let $Z = z/L$ , and $u_z*L/E_z = Pe$

hence

$$c_s(z=1,t) - (1/Pe)*[\partial c(z=1,t)/\partial z] = c_e(z=1,t)$$

Since there exists a discontinuity at this position ,thus

$$c_s(z=1,t) = c_e(z=1,t)$$

So the equation becomes

$$\partial c(z=1,t)/\partial z = 0 \qquad \text{B.4}$$



Let $\hat{c}(z,p) = \mathcal{L}[c(z,t)]$ ; therefore equation B.2 becomes

$$[\mathcal{Z}\{p*\hat{c}(z,p)\}-\{c(z,t=0)\}] = (1/Pe)*[\partial^2\hat{c}/\partial z^2] - \{\partial\hat{c}/\partial z\}$$

Since the initial condition is defined as shown below

$$c(z,t=0) = 0$$

thus

$$\tau * p * \hat{c}(z,p) = (1/Pe)*[\partial^2 \hat{c}(z,p)/\partial z^2] - [\partial \hat{c}(z,p)/\partial z]$$

Let $\hat{\hat{c}}(s,p) = \mathcal{L}[\hat{c}(z,p)]$ ; so

$$\tau * p * \hat{\hat{c}}(s,p) = (1/Pe)*[s^2 \hat{\hat{c}}(s,p) - s\hat{c}(z=0,p) - \{\partial \hat{c}(z=0,p)/\partial z\}] - [s\hat{\hat{c}}(s,p) - \hat{c}(z=0,p)]$$

$$\frac{1}{Pe} * s * \hat{c}(z=0,p) + \frac{1}{Pe} * \frac{\partial \hat{c}(z=0,p)}{\partial z} - \hat{c}(z=0,p) = \frac{1}{Pe} * s^2 * \hat{\hat{c}}(s,p) - s * \hat{\hat{c}}(s,p) - \tau * p * \hat{\hat{c}}(s,p)$$

$$\left(\frac{s^2}{Pe} - s - \tau * p\right) * \hat{\hat{c}}(s,p) = \left(\frac{s}{Pe} - 1\right) * \hat{c}(z=0,p) + (1/Pe) * \frac{\partial \hat{c}(z=0,p)}{\partial z}$$

$$\hat{\hat{c}}(s,p) = \frac{Pe}{(s^2 - sPe - \tau p * Pe)} * -\hat{c}(z=0,p) + s * \frac{\hat{c}(z=0,p)}{Pe} + (1/Pe)\frac{\partial \hat{c}(z=0,p)}{\partial z} \qquad B.5$$

Equation B.3 can be transformed into the Laplace domain as follows

Let $\hat{c}(z,p) = \mathcal{L}[c(z,0)]$

hence

$$\hat{c}_{in}(z=0,p) = \hat{c}(z=0,p) - (1/Pe)*[\partial \hat{c}(z=0,p)/\partial z]$$

or

$$-\hat{c}_{in}(z=0,p) = -\hat{c}(z=0,p) + (1/Pe)*[\partial \hat{c}(z=0,p)/\partial z] \qquad B.6$$

Substituting equation B.6 into B.5

$$\hat{\hat{c}}(s,p) = Pe* \frac{\{s\hat{c}(z=0,p)/Pe\}-\hat{c}_{in}(z=0,p)}{\{s-\lambda_1\}\{s-\lambda_2\}} \qquad B.7$$

where $\lambda_1 = Pe/2 + \sqrt{Pe^2/4 + Pe*p*\tau}$

$\lambda_2 = Pe/2 - \sqrt{Pe^2/4 + Pe*p*\tau}$

Taking the inverse Laplace transform of equation B.7

Let $\hat{c}(z,p) = \mathcal{L}^{-1}[c(s,p)]$

$$\hat{c}(z,p) = Pe* \frac{s}{\{s-\lambda_1\}\{s-\lambda_2\}} *\hat{c}(z=0,p)-Pe*\hat{c}_{in}(z=0,p)* \frac{1}{\{s-\lambda_1\}\{s-\lambda_2\}} \qquad B.8$$

Applying the cover rule and taking the partial fraction to the first term of equation B.8

$$s/[\{s-\lambda_1\}\{s-\lambda_2\}] = a/\{s-\lambda_1\} + b/\{s-\lambda_2\}$$

$$a = \lambda_1/\{\lambda_1-\lambda_2\} \quad \text{and} \quad b = -\lambda_2/\{\lambda_1-\lambda_2\}$$

so

$$s/[\{s-\lambda_1\}\{s-\lambda_2\}] = [\lambda_1/\{\lambda_1-\lambda_2\}]/[s-\lambda_1] - [\lambda_2/\{\lambda_1-\lambda_2\}]/[s-\lambda_2] \qquad B.9$$

Proceeding similarly as above for the second term we obtain

$$1/[\{s-\lambda_1\}\{s-\lambda_2\}] = c/\{s-\lambda_1\} + d/\{s-\lambda_2\}$$

$$c = 1/\{\lambda_1-\lambda_2\} \quad \text{and} \quad d = -1/\{\lambda_1-\lambda_2\}$$

hence

$$1/[\{s-\lambda_1\}\{s-\lambda_2\}] = (1/\{\lambda_1-\lambda_2\})/\{s-\lambda_1\} + [1/\{\lambda_1-\lambda_2\}]/\{s-\lambda_2\} \quad \text{B.10}$$

Applying B.9 and B.10 to B.8, the ultimate equation is

$$\hat{c}(z,p) = \hat{c}(z=0,p)*[(\lambda_1/\{\lambda_1-\lambda_2\})\exp(\lambda_1*z) - (\lambda_2/\{\lambda_1-\lambda_2\})\exp(\lambda_2*z)]$$
$$- Pe*\hat{c}_{in}(z=0,p)*[(1/\{\lambda_1-\lambda_2\})\exp(\lambda_1*z) - (1/\{\lambda_1-\lambda_2\})\exp(\lambda_2*z)]$$

or

$$\hat{c}(z,p) = \frac{Pe}{\{\lambda_1-\lambda_2\}} * (\lambda_1*\exp(\lambda_1*z)-(\lambda_2*\exp(\lambda_2*z)* \frac{\hat{c}(z=0,p)}{Pe}$$
$$- \frac{Pe}{\{\lambda_1-\lambda_2\}} *[\hat{c}_{in}(z=0,p)]*[\exp(\lambda_1*z)-\exp(\lambda_2*z)] \quad \text{B.11}$$



Differentiate B.11 with respect to z



$$\frac{\partial \hat{c}(z,p)}{\partial z} = \frac{Pe}{\{\lambda_1-\lambda_2\}} *[\lambda_1^2*\exp(\lambda_1*z)-\lambda_2^2*\exp(\lambda_2*z)]*[c(z=0,p)/Pe]$$
$$- \frac{Pe}{\{\lambda_1-\lambda_2\}} *[c_{in}(z=0,p)]*[\lambda_1*\exp(\lambda_1*z)-\lambda_2*\exp(\lambda_2*z)] \quad \text{B.12}$$

Transforming B.4 into the Laplace domain and letting $\hat{c}(z,p) = \mathcal{L}[c(z,t)]$

$$\partial \hat{c}(z=1,p)/\partial z \quad = \quad 0 \qquad \text{B.13}$$

Applying B.13 to B.12 at point z=1 we obtain

$$[\lambda_1^2*\exp(\lambda_1*z)-\lambda_2^2*\exp(\lambda_2*z)]*[\hat{c}(z=0,p)/Pe] \quad = \quad [\hat{c}_{in}(z=0,p)]*[\lambda_1*\exp(\lambda_1*z)-\lambda_2*\exp(\lambda_2*z)]$$

or

$$\hat{c}(z=0,p) \quad = \quad \frac{\{\lambda_1*\exp(\lambda_1*z)-\lambda_2*\exp(\lambda_2*z)\}}{\{\lambda_1^2*\exp(\lambda_1*z)-\lambda_2^2*\exp(\lambda_2*z)\}}*[\hat{c}_{in}(z=0,p)]*Pe \qquad \text{B.14}$$

Substituting B.14 into B.11 results in the following

$$\hat{c}(z,p) = [Pe/\{\lambda_1-\lambda_2\}]*[(\lambda_1*\exp(\lambda_1*z)-(\lambda_2*\exp(\lambda_2*z)]*[\hat{c}_{in}(z=0,p)]*[\{\lambda_1*\exp(\lambda_1*z)-\lambda_2*\exp(\lambda_2*z)\}/[\lambda_1^2*\exp(\lambda_1*z)-\lambda_2^2*\exp(\lambda_2*z)] -[Pe/\{\lambda_1-\lambda_2\}]*[\hat{c}_{in}(z=0,p)]*[\exp(\lambda_1*z)-\exp(\lambda_2*z)]$$

or

$$\hat{c}(z,p) = [Pe/\{\lambda_1-\lambda_2\}]*[\hat{c}_{in}(z=0,p)]*[\{-\exp(\lambda_1*z)-\exp(\lambda_2*z)\} + \{\lambda_1*\exp(\lambda_1*z)-\lambda_2*\exp(\lambda_2*z)\}^2/\{\lambda_1^2*\exp(\lambda_1*z)-\lambda_2^2*\exp(\lambda_2*z)\}]$$

Rewriting this in the form of a transfer function

$$\hat{c}(z,p)/\hat{c}_{in}(z=0,p) = [\ ( - \{exp(\lambda_1*z) - exp(\lambda_2*z)\}*\{\lambda_1{}^2*exp(\lambda_1*z) - \lambda_2{}^2*exp(\lambda_2*z) + \{\lambda_1*exp(\lambda_1*z) - \lambda_2*exp(\lambda_2*z)\}^2) / \{\lambda_1{}^2*exp(\lambda_1*z) - \lambda_2{}^2*exp(\lambda_2*z)\}] * [Pe/\{\lambda_1-\lambda_2\}]$$

or

$$\hat{c}(z,p)/\hat{c}_{in}(z=0,p) = [\ (-\lambda_1{}^2*\{exp(2*\lambda_1*z) + \lambda_2{}^2exp(\{\lambda_1+\lambda_2\}*z) + \lambda_1{}^2*exp(\{\lambda_1+\lambda_2\}*z) - \lambda_2{}^2*exp(2*\lambda_2*z) + \lambda_1{}^2*exp(2*\lambda_1*z) + \lambda_2{}^2exp(2*\lambda_2 z) - \lambda_2*\lambda_1*\lambda_2*exp(\{\lambda_1+\lambda_2\}*z)) / \{\lambda_1{}^2*exp(\lambda_1*z)-\lambda_2{}^2*exp(\lambda_2*z)\}] * [Pe/\{\lambda_1-\lambda_2\}]$$

Rewriting the above transfer function yields

$$\frac{\hat{c}(z,p)}{\hat{c}_{in}(z=0,p)} = \frac{\{\lambda_1-\lambda_2\}^2*exp(\{\lambda_1+\lambda_2\}*z)}{\{\lambda_1{}^2*exp(\lambda_1*z)-\lambda_2{}^2*exp(\lambda_2*z)\}} * \frac{Pe}{\{\lambda_1-\lambda_2\}}$$

or

$$\frac{\hat{c}(z,p)}{\hat{c}_{in}(z=0,p)} = Pe* \frac{\{\lambda_1-\lambda_2\}*exp(\{\lambda_1+\lambda_2\}*z)}{\{\lambda_1{}^2*exp(\lambda_1*z)-\lambda_2{}^2*exp(\lambda_2*z)\}}$$

$$= \frac{Pe*\{\ _1-\ _2\}}{exp(-\{\lambda_1+\lambda_2\}*z)*\{\lambda_1{}^2*exp(\lambda_1*z)-\lambda_2{}^2*exp(\lambda_2*z)\}]}$$

Thus

$$\frac{\hat{c}(z,p)}{\hat{c}_{in}(z=0,p)} = \frac{Pe*\{\lambda_1-\lambda_2\}}{\{\lambda_1^2*\exp(-\lambda_2*z)-\lambda_2^2*\exp(-\lambda_1*z)\}} \qquad B.15$$

At the end of the bed column at Z=1 the transfer function eventually becomes

$$H(p) = \frac{\hat{c}(z=1,p)}{\hat{c}_{in}(z=0,p)} = \frac{Pe*\{\lambda_1-\lambda_2\}}{\{\lambda_1^2*\exp(-\lambda_2)-\lambda_2^2*\exp(-\lambda_1)\}} \qquad B.16$$

# APPENDIX C

## SIMPLIFICATION OF MODEL'S TRANSFER FUNCTION TO COMPLEX FORM

$$H(j\omega) = \frac{Pe\left[\lambda_1 - \lambda_2\right]}{\lambda_1^2 \cdot e^{-\lambda_2} - \lambda_2^2 \cdot e^{-\lambda_1}} \qquad \text{C.1}$$

$$\lambda_1, \lambda_2 = \frac{1}{2}\left[Pe + \sqrt{Pe^2 + 4 \cdot Pe \cdot \tau \cdot j \cdot \omega}\right]$$

Let $a = Pe$ $\qquad b = 4 \cdot \omega \cdot \tau$

$$r = \sqrt{a^4 + a^2 \cdot b^2} \qquad \theta = \tan^{-1}\frac{b}{a}$$

Therefore

$$\lambda_1 = \frac{1}{2}\left[a + \sqrt{a^2 + a \cdot b \cdot j}\right]$$

$$\frac{1}{2}\left[a + \left[\sqrt{r} \cdot \cos\left[\frac{\theta}{2}\right] + j \cdot \sqrt{r} \cdot \sin\left[\frac{\theta}{2}\right]\right]\right]$$

$$\left[\frac{1}{2} \cdot a + \frac{1}{2} \cdot \sqrt{r} \cdot \cos\left[\frac{\theta}{2}\right]\right] + j \cdot \sqrt{r} \cdot \sin\left[\frac{\theta}{2}\right]$$

$$\lambda_2 = \frac{1}{2}\left[a - \sqrt{a^2 + a \cdot b \cdot j}\right]$$

$$\frac{1}{2}\left[a - \sqrt{r} \cdot \cos\left[\frac{\theta}{2}\right] + j \cdot \sqrt{r} \cdot \sin\left[\frac{\theta}{2}\right]\right]$$

$$\left[\frac{1}{2} \cdot a - \frac{1}{2} \cdot \sqrt{r} \cdot \cos\left[\frac{\theta}{2}\right]\right] + j \cdot \sqrt{r} \cdot \sin\left[\frac{\theta}{2}\right]$$

Now defining the following term as

$$c = \frac{1}{2}\left[a + \sqrt{r} \cdot \cos\left[\frac{\theta}{2}\right]\right]$$

$$d = \frac{1}{2}\left[a - \sqrt{r} \cdot \cos\left[\frac{\theta}{2}\right]\right]$$

$$l = \frac{1}{2}\left[\sqrt{r} \cdot \sin\left[\frac{\theta}{2}\right]\right]$$

Hence

$$\lambda_1 = c + j \cdot l \qquad \text{C.2}$$

$$\lambda_2 = d - j \cdot l \qquad \text{C.3}$$

Let $f = \left[c^2 - 1^2\right]$ ; $h = \left[d^2 + 1^2\right]$

$g = 2 \cdot c \cdot 1$ ; $k = 2 \cdot d \cdot 1$

Thus

$$\lambda_1^2 = (c + j \cdot 1)^2 = \left[c^2 - 1^2\right] + j \cdot 2 \cdot c \cdot 1 = f + j \cdot g \qquad C.4$$

$$\lambda_2^2 = (d + j\ 1)^2 = \left[d^2 + 1^2\right] + 2 \cdot d \cdot 1 \cdot j = h + j \cdot k \qquad C.5$$

for $m = e^{-c} \cos(1)$ ; $n = e^{-c} \sin(1)$

$o = e^{-d} \cos(1)$ ; $q = e^{-d} \sin(1)$

Then

$$e^{-\lambda_1} = e^{-c-j \cdot 1} = e^{-c} \cdot (\cos(1) - j \cdot \sin(1)) = m - j \cdot n \qquad C.6$$

$$e^{-\lambda_2} = e^{-d+j \cdot 1} = e^{-d} \cdot (\cos(1) + j \cdot \sin(1)) = o + j \cdot q \qquad C.7$$

Substituting c.2 , c.3 , c.4 , c.5 , c.6 , c.7 in c.1

$$H(j\omega) = Pe \cdot \frac{c - d - j \cdot 2 \cdot 1}{(f + j \cdot g) \cdot (o + jq) - (h + j \cdot k) \cdot (m - j \cdot n)}$$

$$= Pe \cdot \left[\frac{c - d + j \cdot 2 \cdot 1}{(f \cdot o - g \cdot q - h \cdot m - n\ k) + j(f \cdot q + g \cdot o + h \cdot n - m \cdot k)}\right]$$

Let $t = f \cdot o - g \cdot q - h \cdot m - n \cdot k$

$s = f \cdot q + g \cdot o + h \cdot n - m \cdot k$

therefore equation c.1 eventually becomes

$$H(j\omega) = Pe \cdot \left[\frac{(c - d) + 2 \cdot j \cdot 1}{t + j \cdot s}\right] \cdot \left[\frac{t - i \cdot s}{t - i \cdot s}\right]$$

$$= Pe \cdot \left[\frac{(c - d) \cdot t + 2 \cdot s \cdot 1}{t^2 + s^2}\right] + j \cdot \left[\frac{-(c - d) \cdot s + 2 \cdot 1 \cdot t}{t^2 + s^2}\right]$$

$$= Re + jIm$$

Where $Re = \left[\frac{Pe}{t^2 + s^2}\right] \cdot ((c - d) \cdot t + 2 \cdot 1 \cdot s)$

$Im = \left[\frac{Pe}{t^2 + s^2}\right] \cdot (-(c - d) \cdot s + 2 \cdot 1 \cdot t)$

# APPENDIX D

## CURVE FITTING BETWEEN THEORETICAL RELATION AND EXPERIMENTAL DATA

Let the following notations be defined as follows :

| | | |
|---|---|---|
| Pe | = | Peclet Number |
| $\tau$ | = | mean residence time |
| N | = | number of sampling points |
| $\omega$ | = | frequency |
| i | = | sampling points in the frequency domain |
| $H_i$ | = | transfer function at the $i^{th}$ point |
| $H_i$ | = | amplitude of transfer function at point $i^{th}$ |
| $arg[H_i]$ | = | argument of transfer function at point $i^{th}$ |
| k | = | sampling point in time domain |
| F | = | normalized theoretical function in time domain obtained from inversion of transfer function by Inverse Fourier transformation |
| T | = | theoretical time |
| r | = | sampling point of experimental data |
| $g_r$ | = | experimental data at $r^{th}$ |
| f | = | normalized experimental function |
| t | = | experimental time |

The following curve fitting exercises for three different flow rates illustrate how suitable the proposed model based on Pe and $\tau$ obtained from experiment is .

## D.1 Curve fitting at high velocity

The following presentation shows plots of magnitude , phase angle and transfer function against frequencies .

$$Pe := 208$$

$$\tau := 50.53148$$

$$N := 64$$

$$d\omega := 0.038$$

$$i := 0 \,..N$$

$$\omega_i := i \cdot d\omega$$

$$\lambda1_i := 0.5 \cdot \left[ Pe + \sqrt{Pe^2 + 4 \cdot Pe \cdot \tau \cdot \omega_i \cdot j} \right]$$

$$\lambda2_i := Pe - \lambda1_i$$

$$H_i := \left[ \frac{Pe \cdot \left[\lambda1_i - \lambda2_i\right]}{\left[\left[\lambda1_i \cdot \lambda1_i\right] \cdot \exp\left[-\lambda2_i\right]\right] - \left[\left[\lambda2_i \cdot \lambda2_i\right] \cdot \exp\left[-\lambda1_i\right]\right]} \right]$$

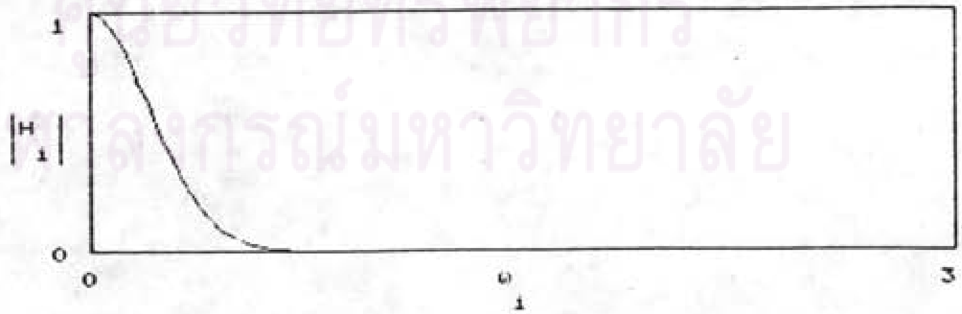


Fig. D1 Curve showing magnitude of transfer function vs frequency for Pe = 208 and $\tau$ = 50.53148

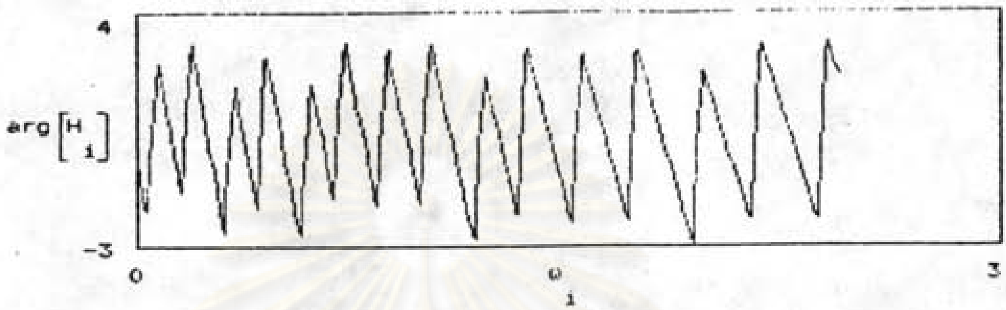


Fig. D2 The Argument of Transfer Function vs Frequency for Pe = 208 and $\tau$ = 50.53148

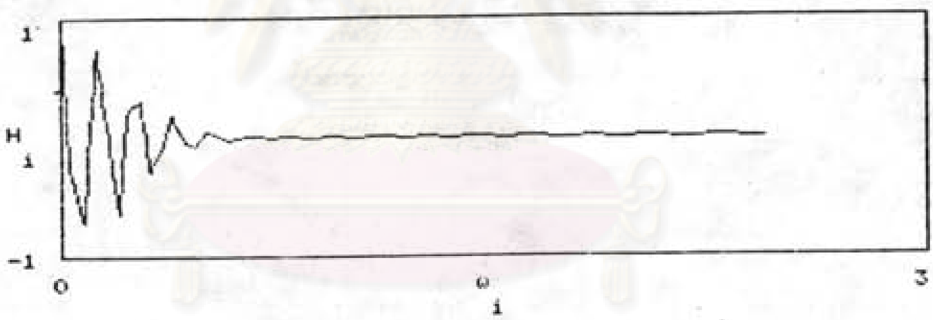


Fig. D3 Curve of Transfer Function vs Frequency for Pe = 208 and $\tau$ = 50.53148

The transformation of the functions from the frequency domain to the time domain can be performed in the following manner .

$k := 0 \,..\, 127$

$F := 0.0598 \cdot \mathrm{ifft}\left[H\right]$

$T_k := k \cdot \dfrac{2 \cdot \pi}{2 \cdot N \cdot d\omega}$

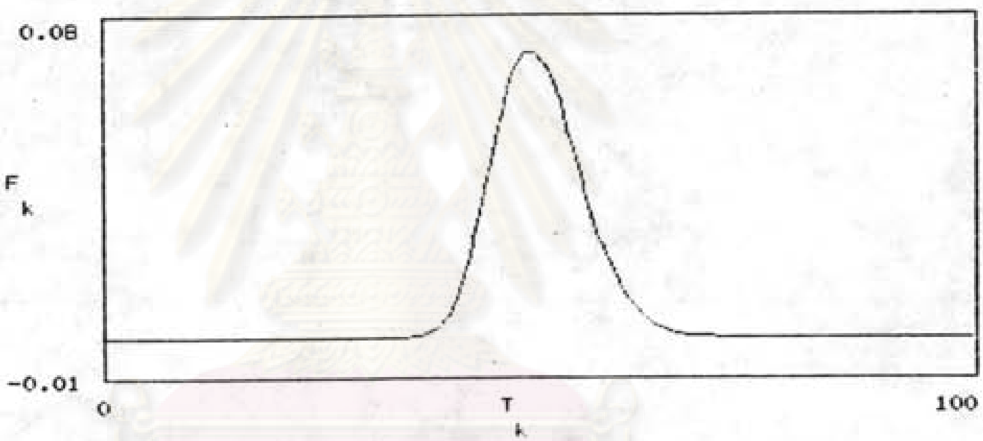


Fig. D4 Theoretical Normalized Concentration-time Curve for Pe = 208 and $\tau$ = 50.53148



The experimental concentration distribution data and the comparison of the experimental response curve with the theoretical curve are presented as follows :-

$r := 1 .. 42$

| $g_r :=$ | $t_r :=$ |
|---|---|
| 0 | 35.4 |
| 2 | 36.285 |
| 3.5 | 37.17 |
| 5 | 38.055 |
| 7.5 | 38.94 |
| 10.5 | 39.825 |
| 19 | 40.71 |
| 26 | 41:595 |
| 36 | 42.48 |
| 45 | 43.365 |
| 60.5 | 44.25 |
| 85.5 | 45.135 |
| 97 | 46.02 |
| 109 | 46.905 |
| 120 | 47.79 |
| 133 | 48.675 |
| 137 | 49.56 |
| 139 | 50.445 |
| 136.5 | 51.33 |
| 132.5 | 52.215 |
| 119.5 | 53.1 |
| 109.5 | 53.985 |
| 96.5 | 54.87 |
| 84.5 | 55.755 |
| 72 | 56.64 |
| 58 | 57.525 |
| 45 | 58.41 |
| 31 | 59.295 |
| 11 | 60.18 |
| 5 | 61.065 |
| 4 | 61.95 |
| 3 | 62.835 |
| 2.5 | 63.72 |
| 2 | 64.605 |
| 1.5 | 65.49 |
| 1 | 66.375 |
| 1 | 67.26 |
| 1 | 68.145 |
| 0.5 | 69.03 |
| 0.5 | 69.915 |
| 0.5 | 70.8 |
| 0.5 | 71.685 |

$f_r := 0.00051164\ g_r$

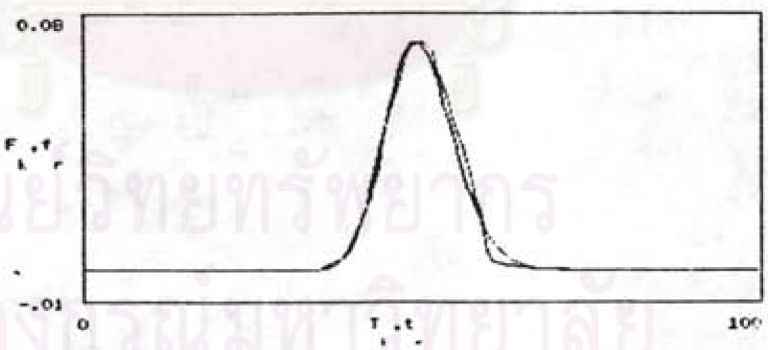


Fig. D5 Comparison of experimental response curve and theoretical response for Pe = 208 and $\tau$ = 50.53148

## D.2 Curve fitting at medium velocity

The following presentation shows the plots of magnitude , phase angle and transfer function against frequencies .

$$Pe := 230$$

$$\tau := 82.39171$$

$$N := 64$$

$$d\omega := 0.019$$

$$i := 0 \,..N$$

$$\omega_i := i \cdot d\omega$$

$$\lambda1_i := 0.5 \cdot \left[ Pe + \sqrt{Pe^2 + 4 \cdot Pe \cdot \tau \cdot \omega_i \cdot j} \right]$$

$$\lambda2_i := Pe - \lambda1_i$$

$$H_i := \left[ \frac{Pe \cdot \left[ \lambda1_i - \lambda2_i \right]}{\left[ \left[ \lambda1_i \cdot \lambda1_i \right] \cdot \exp\left[ -\lambda2_i \right] \right] - \left[ \left[ \lambda2_i \cdot \lambda2_i \right] \cdot \exp\left[ -\lambda1_i \right] \right]} \right]$$

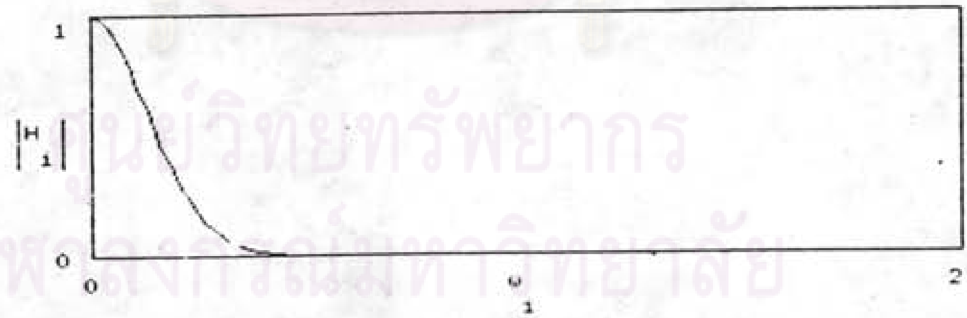




Fig. D6 Curve showing magnitude of transfer function vs frequency for Pe = 230 and $\tau$ = 82.39171

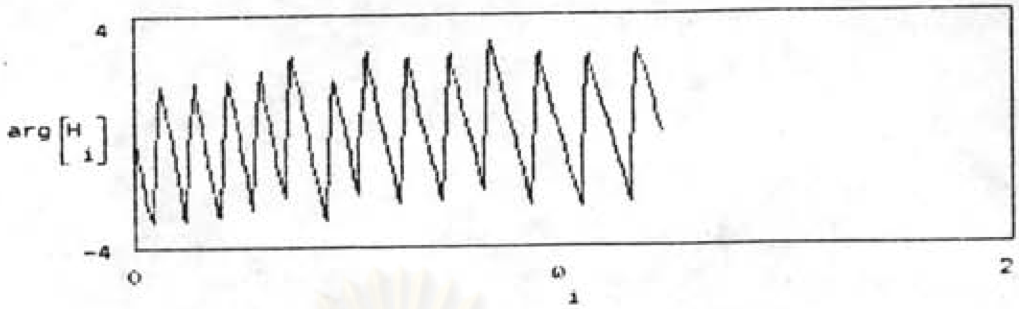


Fig. D7 The Argument of Transfer Function vs Frequency for Pe = 230 and $\tau$ = 82.39171

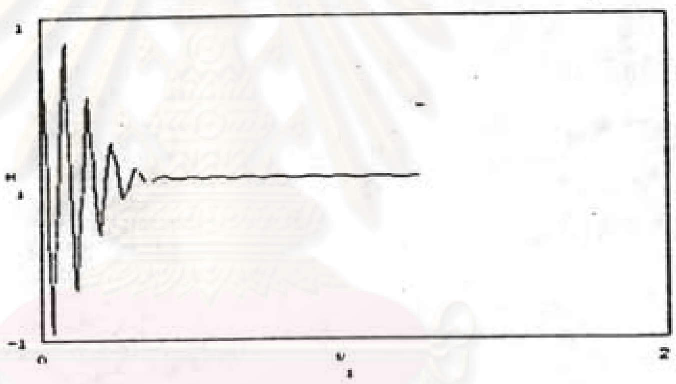


Fig. D8 Curve of Transfer Function vs Frequency for Pe = 208 and $\tau$ = 50.53148

The transformation of the functions from the frequency domain to the time domain can be performed in the following manner .

$$k := 0\ ..127$$

$$F := 0.0723 \cdot \mathrm{ifft}\left[H\right]$$

$$T_k := k \cdot \frac{2 \cdot \pi}{2 \cdot N \cdot d\omega}$$

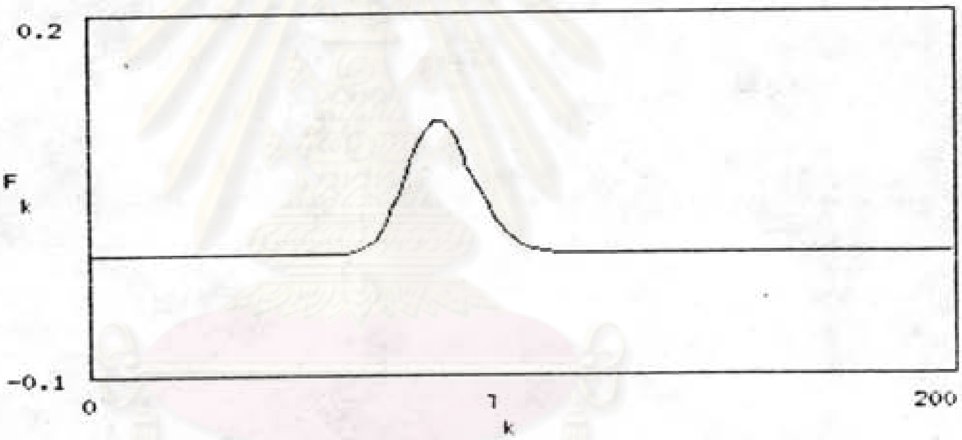


Fig. D9 Theoretical Normalized Concentration-time Curve for Pe = 230 and $\tau$ = 82.39171



The experimental concentration distribution data and the comparison of the experimental response curve with the theoretical curve are presented as follows :-

## D.3 Curve fitting at low velocity

The following presentation shows the plots of magnitude , phase angle and transfer function gainst frequencies .

$Pe := 260$

$\tau := 209.0635$

$N := 64$

$d\omega := 0.012$

$i := 0 .. N$

$\omega_i := i \cdot d\omega$

$$\lambda1_i := 0.5 \cdot \left[ Pe + \sqrt{Pe^2 + 4 \cdot Pe \cdot \tau \cdot \omega_i \cdot j} \right]$$

$\lambda2_i := Pe - \lambda1_i$

$$H_i := \left[ \frac{Pe \cdot \left[ \lambda1_i - \lambda2_i \right]}{\left[ \left[ \lambda1_i \cdot \lambda1_i \right] \cdot \exp\left[ -\lambda2_i \right] \right] - \left[ \left[ \lambda2_i \cdot \lambda2_i \right] \cdot \exp\left[ -\lambda1_i \right] \right]} \right]$$

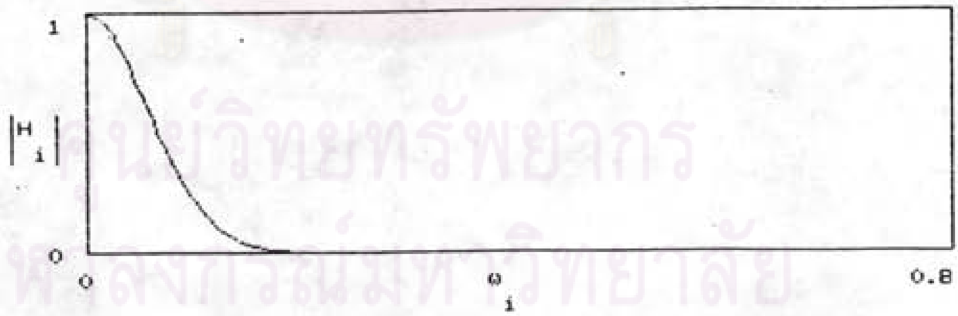


Fig. D11 Curve showing magnitude of transfer function vs frequency for Pe = 260 and $\tau$ = 209.0635

## D.3 Curve fitting at low velocity

The following presentation shows the plots of magnitude , phase angle and transfer function gainst frequencies .

$$Pe := 260$$

$$\tau := 209.0635$$

$$N := 64$$

$$d\omega := 0.012$$

$$i := 0 \,..N$$

$$\omega_i := i \cdot d\omega$$

$$\lambda1_i := 0.5 \cdot \left[ Pe + \sqrt{Pe^2 + 4 \cdot Pe \cdot \tau \cdot \omega_i \cdot j} \right]$$

$$\lambda2_i := Pe - \lambda1_i$$

$$H_i := \left[ \frac{Pe \cdot \left[ \lambda1_i - \lambda2_i \right]}{\left[ \left[ \lambda1_i \cdot \lambda1_i \right] \cdot \exp\left[ -\lambda2_i \right] \right] - \left[ \left[ \lambda2_i \cdot \lambda2_i \right] \cdot \exp\left[ -\lambda1_i \right] \right]} \right]$$

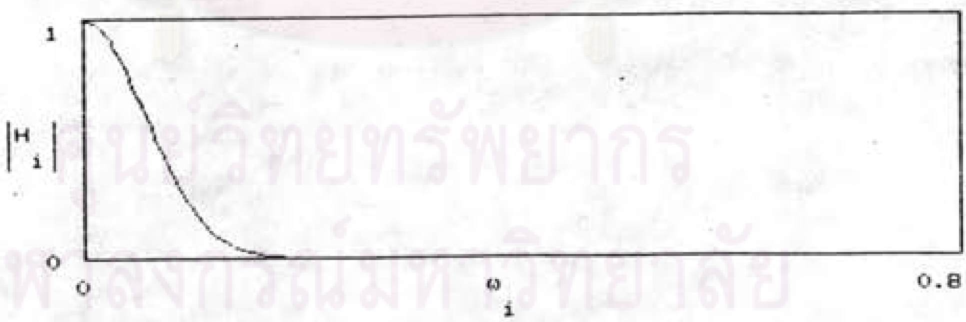


Fig. D11 Curve showing magnitude of transfer function vs frequency for Pe = 260 and $\tau$ = 209.0635

$k := 0 \,..127$

$F := 0.034\ \mathrm{ifft}(H)$

$T_k := k \dfrac{2\pi}{2 \cdot N \cdot d\omega}$

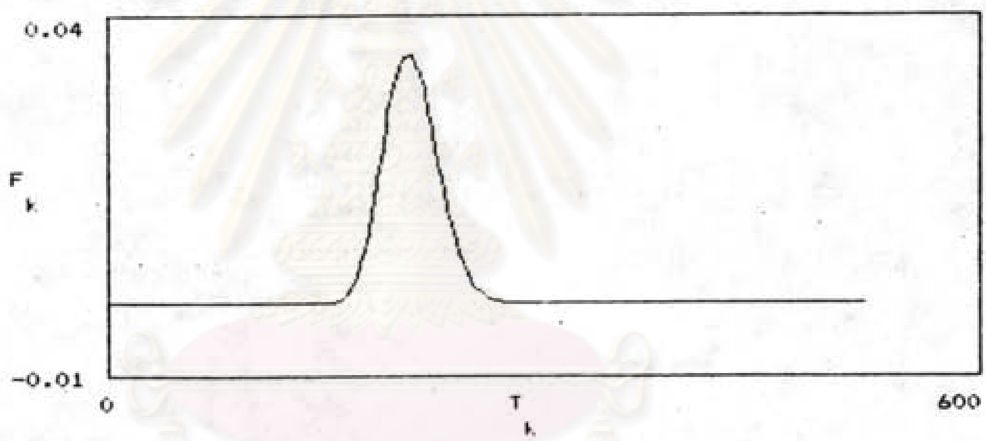


Fig. D14 Theoretical Normalized Concentration-time Curve for Pe = 260 and $\tau$ = 209.0635



The experimental concentration distribution data and the comparison of the experimental response curve with the theoretical curve are presented as follows :-

$r := 0 .. 77$

| $g0_r :=$ | $g50_r :=$ | $t0_r :=$ | $t50_r :=$ |
|---|---|---|---|
| 0.5 | 68 | 146.4 | 228.8551 |
| 0.5 | 63 | 148.0827 | 230.5379 |
| 0.5 | 56 | 149.7655 | 232.2206 |
| 0.5 | 52 | 151.4482 | 233.9034 |
| 1 | 50 | 153.1310 | 235.5862 |
| 1 | 43 | 154.8137 | 237.2689 |
| 1.5 | 39 | 156.4965 | 238.9517 |
| 1.5 | 34 | 158.1793 | 240.6344 |
| 2 | 29 | 159.8620 | 242.3172 |
| 2.5 | 25 | 161.5448 | 244 |
| 4.5 | 22 | 163.2275 | 245.6827 |
| 6 | 18 | 164.9103 | 247.3655 |
| 8.5 | 15 | 166.5931 | 249.0482 |
| 10 | 11 | 168.2758 | 250.7310 |
| 13.5 | 8 | 169.9586 | 252.4137 |
| 17 | 6 | 171.6413 | 254.0965 |
| 18.5 | 4 | 173.3241 | 255.7793 |
| 22 | 2.5 | 175.0068 | 257.4620 |
| 27 | 2 | 176.6896 | 259.1448 |
| 33 | 2 | 178.3724 | 260.8275 |
| 40 | 2 | 180.0551 | 262.5103 |
| 46.5 | 1.5 | 181.7379 | 264.1931 |
| 53 | 1 | 183.4206 | 265.8758 |
| 60 | 1 | 185.1034 | 267.5586 |
| 66 | 0.5 | 186.7862 | 269.2413 |
| 72 | 0.5 | 188.4689 | 270.9241 |
| 78 | 0.5 | 190.1517 | 272.6068 |
| 86 | 0.5 | 191.8344 | 274.2896 |
| 91 | 0.5 | 193.5172 | 275.9724 |
| 97.5 | | 195.2 | |
| 103 | | 196.8827 | |
| 105.5 | | 198.5655 | |
| 109.5 | | 200.2482 | |
| 112 | | 201.9310 | |
| 113.5 | | 203.6137 | |
| 115 | | 205.2965 | |
| 115.5 | | 206.9793 | |
| 116.5 | | 208.6620 | |
| 115.5 | | 210.3448 | |
| 114 | | 212.0275 | |
| 112 | | 213.7103 | |
| 109.5 | | 215.3931 | |
| 106 | | 217.0758 | |
| 100 | | 218.7586 | |
| 95 | | 220.4413 | |
| 89 | | 222.1241 | |
| 85 | | 223.8068 | |
| 80 | | 225.4896 | |
| 75 | | 227.1724 | |

$$q_r := \mathrm{if}\left[r \le 48, g0_r, g50_{r-49}\right]$$

$$t_r := \mathrm{if}\left[r \le 48, t0_r, t50_{r-49}\right]$$

$$f_r := 0.00029477\, q_r$$

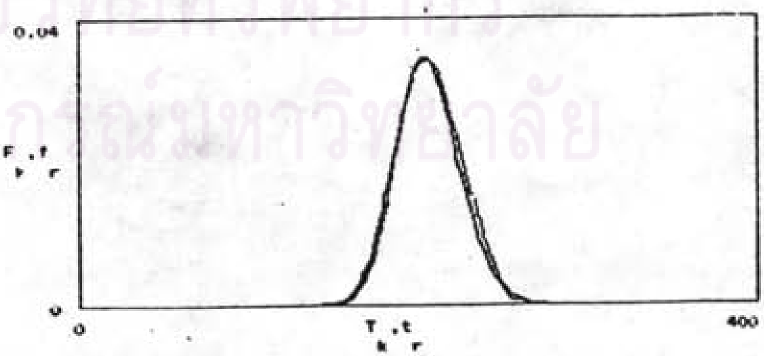


Fig.D15 Comparison of experimental response curve and theoretical response for Pe = 260 and $\tau$ = 209.0635

# APPENDIX E

## MOMENT'S METHOD FOR DERIVATION OF MEAN RESIDENCE TIME AND VARIANCE

From the transfer function given in equation 2.6

$$H(s) = \frac{Pe*(\lambda_1-\lambda_2)}{[\lambda_1^{2}*\exp(-\lambda_2) - \lambda_2^{2}*\exp(-\lambda_1)]}$$

let $q = \sqrt{1 + 4s/Pe}$ , $U = (Pe/2)*(1+q)$ , $V = (Pe/2)*(1-q)$

$$H(s)_{z=1} = \frac{Pe*[(Pe/2)*(2*q)]}{\frac{Pe^2}{4}*(1+q)^2*e^{-(Pe/2)*(1-q)} - \frac{Pe^2}{4}*(1-q)^2*e^{-(Pe/2)*(1+q)}}$$

$$= \frac{4*q*e^{[(Pe/2)*(1-q)]}}{[(1+q)^2 - (1-q)^2*e^{(-\{Pe/e\}*\{1+q\}+\{Pe/2\}*\{1-q\})}]}$$

$$= \frac{4*q*e^{V}}{[(1+q)^2 - (1-q)^2*e^{(-U+V)}]} \qquad \text{E.1}$$

Therefore equation E.1 eventually becomes

$$H(s) = \frac{4*q*\exp(\{Pe/2\}*\{1-q\})}{[(1+q)^2 - (1-q)^2*\exp(-Pe*q)]} \qquad E.2$$

since

$$\frac{dH}{ds} = \frac{dH}{dq}.\frac{dq}{ds}$$

and

$$\frac{dq}{ds} = \frac{1}{2}(1 + 4s\ /Pe)^{-1/2}(4\ /Pe) = \frac{2\tau}{Pe\sqrt{1+4s\tau/Pe}} = 2\tau/Pe$$

$$\frac{dH}{dq} = 4\left[\frac{[(1+q)^2-(1-q)^2*e^{-Pe*q}][-q*\{Pe/2\}*e^{\{Pe/2\}*(1-q)}+e^{\{Pe/2\}*\{1-q\}}]}{[(1+q)^2 - (1-q)^2*e^{-Pe*q}]^2}\right]$$

$$-4\left[\frac{[q*e^{\{Pe/2\}*\{1-q\}}][2*(1+q)-\{-2(1-q)e^{-Pe*q}+(1-q)^2*(-Pe)*e^{-Pe*q}\}]}{[(1+q)^2 - (1-q)^2*e^{-Pe*q}]^2}\right]$$

Thus

$$\frac{dH}{dq}.\frac{dq}{ds} = \frac{8*\tau}{Pe*q}\left[\frac{[(1+q)^2-(1-q)^2e^{-Pe*q}][q*Pe/2*e^{\{Pe/2\}\{1-q\}}+e^{\{Pe/2\}\{1-q\}}]}{[(1+q)^2 - (1-q)^2*e^{-Pe*q}]^2}\right]$$

$$-\frac{8*\tau}{Pe*q}\left[\frac{[q*e^{\{Pe/2\}*\{1-q\}}][2*(1+q)-\{-2(1-q)e^{-Pe*q}+(1-q)^2*(-Pe)*e^{-Pe*q}\}]}{[(1+q)^2 - (1-q)^2*e^{-Pe*q}]^2}\right]$$

or

$$\frac{dH}{ds} = \tau \frac{[(1+q)^2-(1-q)^2 e^{-Pe*q}][\{(8/Pe*q)-4\}*e^{\{Pe/2\}\{1-q\}}]}{[(1+q)^2 - (1-q)^2 * e^{-Pe*q}]^2}$$

$$- \tau \left[ \frac{[4*q*e^{\{Pe/2\}*\{1-q\}}] \; \frac{4*(1+q)}{Pe*q} - \{\frac{-2(1-q)e^{-Pe*q}}{Pe*q} + (1-q)^2*(2/q)*e^{-Pe*q}\}}{[(1+q)^2 - (1-q)^2 * e^{-Pe*q}]^2} \right]$$

$$\lim_{s \to 0} \frac{-dH}{ds} = \left[\frac{-(2)^2[\{8/Pe\}-4] + 4(8/Pe)}{(2)^4}\right]$$

$$= \left[\frac{-32/Pe + 16 + 32/Pe}{16}\right]$$

$$= \tau \qquad \text{E.3}$$

According to equation 3.36

$$\mu_1 = \bar{t} = \tau$$

let the following letters be defined as :

$$G = \frac{4*(1+q)}{Pe*q} - \{\frac{-2(1-q)e^{-Pe*q}}{Pe*q} + (1-q)^2*(2/q)*e^{-Pe*q}$$

$$H = e^{\{Pe/2\}\{1-q\}}$$

$$I = \{(8/Pe*q)-4\}$$

$$J = [(1+q)^2-(1-q)^2 e^{-Pe*q}]$$

$$K = H*I*J$$

$$L = 4*q*H*G$$

$$M = e^{[-Pe*q+\{Pe/2\}\{1-q\}]}$$

Therefore the second order differentiation of the transfer function is

$$\frac{\partial^2 H}{\partial s^2} = \frac{(\partial H/\partial s)}{\partial s} = \frac{J^2*\left[\frac{\tau\partial K}{\partial s} - \frac{\tau\partial L}{\partial s}\right]}{(J^2)^2} - \left[\frac{K-L}{J^4}\right]\tau\frac{\partial J^2}{\partial s} \qquad \text{E.4}$$

Now consider the following differentiations

$$\frac{\partial K}{\partial s} = J*\frac{\partial I*H}{\partial s} + I*H*\frac{\partial J}{\partial s}$$

$$= J*[\ I*H*\{-\tau/q\} - \{16\tau/Pe^2*q^3\}*H\ ] + I*H*G*\tau \qquad \text{E.5}$$

$$-\frac{\partial L}{\partial s} = -\frac{\partial\{16/Pe\}*H}{\partial s} + \frac{\partial\{16*q/Pe\}*H}{\partial s} - \frac{\partial 8*M}{\partial s} + \frac{\partial 16*q*M}{\partial s}$$

$$\frac{\partial 8*q^2*M}{\partial s} - \frac{\partial\{16/Pe\}*M}{\partial s} + \frac{\partial\{16*q/Pe\}*M}{\partial s}$$

$$= \{\tau*16/(Pe*q)\}*H + \{\tau*16/Pe\}*H - \{\tau*32/(Pe^2*q)\}*H + \{\tau*24/q\}*M - \{48*\tau\}*M + \{\tau*32/(Pe*q)\}*M + 24*\tau*q*M - \{\tau*32/Pe\}*M + \{\tau*48/(Pe*q)\}*M - \{\tau*48/Pe\}*M + \{32/(Pe^2*q)\}*M \quad E.6$$

$$\frac{\partial J^2}{\partial s} = 2*J*\tau*G \quad E.7$$

Substituting E.5 to E.7 into E.4 , then taking the limit of such a relationship . As s approaches zero , we obtain

$$\lim_{s\to 0}\frac{\partial^2 H}{\partial s^2} = \frac{\tau\partial J^2}{(J^2)^2} * \lim_{s\to 0}\frac{\partial K}{\partial s} - \frac{\tau J^2}{(J^2)^2} * \lim_{s\to 0}\frac{\partial L}{\partial s} -$$

$$\tau\frac{K - L}{J^4} * \lim_{s\to 0}\frac{\partial J^2}{\partial s}$$

$$= -\frac{4*\tau^2}{Pe} + \tau^2 + \frac{2*\tau^2}{Pe} - \frac{2*\tau^2}{Pe^2} + \frac{2*\tau^2*e^{-Pe}}{Pe^2} + \frac{4*\tau^2}{Pe} \quad E.8$$

By substracting E.3 from E.8 , this yields equation 3.37 .

$$\sigma^2 = \frac{2*\tau^2}{Pe} - \frac{2*\tau^2}{Pe^2} + \frac{2*\tau^2*e^{-Pe}}{Pe^2} \qquad E.9$$

## APPENDIX F

### DETERMINATION OF PARTICLE SIZES

The crushed particles were sieved with 30 - 50 mesh screens and determined by a microscope with a spectromicrometer . By using Ferret's method as depicted in figure F1, the particle size distributions appear to have the same shape as in figure F2. The surface mean diameters with the following relationship were utilized to obtain the average diameter .

$$\text{surface mean diameter} = d_{p\Sigma n} = \left(\frac{\Sigma n d_p^2}{\Sigma n}\right)^{0.5}$$

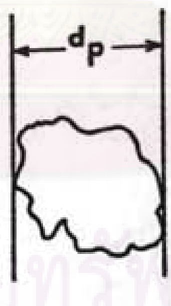


Fig.F1 Ferret's diameter , must be the longest dimension along the line parallel to the base of the field of view

The obtained surface mean diameters were 0.4919 , 0.6314 , 0.8075 and 0.986 mm .



Fig.F.2 Particle size distribution with an average of 0.6314 mm .

# APPENDIX G

## SAMPLE CALCULATIONS

The following sample calculations are based on system H-4-0.9 at volumetric flow rate 0.81 cc/sec

1. Calculation for Density of Propane

From $$PV = nRT$$

$$P = \left(\frac{m}{V}\right)*\left(\frac{R}{MW.}\right)*T = \rho*K*T$$

At constant pressure : $$\rho_1 T_1 = \rho_2 T_2$$

$$\rho_{propane(0\,^\circ c,1\ atm)} = 1.97 \times 10^{-3} \quad g/cc^{(G.1)}$$

so $$\rho_{propane(45\,^\circ c,1\ atm)} = \frac{(1.97 \times 10^{-3})(273.15)}{318.15}$$

$$= 1.691 \times 10^{-3} \quad g/cc$$

$$= 1.691 \quad Kg/m^3$$



---

G.1/ Data obtained from Handbook of tables for Applied Engineering Science , 2nd ed., The Chemical Rubber Co., 1973 , pp. 57 .

2. Calculation for Superficial Velocity

$$U = Q/A = \frac{Q}{(\pi/4)^{*}d_t^2}$$

For $Q = 10/12.38 = 0.81$ cc/sec

$d_t = 0.45$ inch $= 1.14$ cm

Thus $U = \frac{0.8078}{(0.7854)(1.14)^2} = 0.7936$ cm/sec

$= 7.936 \times 10^{-3}$ m/sec

3. Calculation for Reynolds Numbers

From $Re = \frac{U\rho d_p}{\mu}$

$\mu_{propane(45°c,1 atm)} = 0.875 \times 10^{-2}$ $cp^{(G.2)}$

$= 8.75 \times 10^{-6}$ Pa*sec

$d_p = 0.9861$ mm

$= 9.861 \times 10^{-4}$ m

so $Re = \frac{(7.936 \times 10^{-3})(1.691)(9.861 \times 10^{-4})}{(8.75 \times 10^{-6})}$

$= 1.5124$

4. Calculation for The Mean Residence Time

From equation 3.30 , 3,36

$$\mu_{ty} = \frac{\Sigma t c_e(t)\Delta t}{\Sigma c_e(t)\Delta t} = \Sigma t\left(\frac{c_e(t)}{\Sigma c_e(t)}\right)$$

$$= \Sigma t F_y(t) = -\lim_{s \to 0} \frac{dY(s)}{ds}$$

$$\mu_{ty} = -\lim_{s \to 0} \frac{dH(s)}{ds} = \bar{t}$$

From value in table G.1

$$\Sigma c_e(t) = 1954.5$$

and $\mu_{packed\ bed} = 50.53$

A similar calculation for $\mu_{blank}$ is done by using data in table G.2

so $\mu_{blank} = 2.56$



-----------------------------------

G.2/ Data from monograph in Perry Handbook pp.21 .

5. Calculation for The Variance

From equation 3.31

$$\sigma^2_{ty} = \frac{\Sigma(t-\mu)^2 c_e(t)\Delta t}{\Sigma c_e(t)\Delta t} = \Sigma(t-\mu_{ty})^2\left(\frac{c_e(t)}{\Sigma c_e(t)}\right)$$

$$= \Sigma(t-\mu_{ty})^2 F_y(t) = \lim_{s\to 0}\left[\frac{d^2Y(s)}{ds^2} - \left(\frac{dY(s)}{ds}\right)^2\right]$$

From table G.1

Hence $\sigma^2_{\text{packed bed}} = 23.06$

A similar calculation for $\sigma^2_{\text{blank}}$ is done by using data obtained from table G.1

therefore $\sigma^2_{\text{blank}} = 1.04$

6. Calculation for The Peclet Number

From equation 3.37

$$\frac{\sigma^2}{\bar{t}^2} = \frac{2}{Pe} - \frac{2}{Pe^2} + \frac{2}{Pe^2} * e^{-Pe}$$

$$\sigma^2 = \sigma^2_{\text{packed bed}} - \sigma^2_{\text{blank}}$$

$$= 23.06 - 1.04$$

$$= 22.02$$

$$\bar{t}^2 = (t_{packed\ bed} - t_{blank})^2$$

$$= (50.53 - 2.56)^2$$

$$= 2301.12$$

Using the program shown in appendix H , the Peclet value obtained was 208

7. Calculation for Axial Dispersion

From $E_z = U*L/Pe$

where $L = 6.0 \times 10^{-1}$ cm

Then

$$E_z = \frac{(7.936 \times 10^{-3})(6.0 \times 10^{-1})}{(208)}$$

$$= 2.289 \times 10^{-5} \ m^2/sec$$

$$= 0.2289 \ cm^2/sec$$

8. Calculation for Particle Peclet Number

$$Pe_p = \frac{U*d_p}{E_z}$$

$$= \frac{(7.936 \times 10^{-3})(9.861 \times 10^{-4})}{(2.289 \times 10^{-5})}$$

$$= 0.3419$$

Table G.1 Data , mean and variance for sample calculation

| t (sec) | $C_e(t)$ | $F_v(t)$ | $tF_v(t)$ | $(t-\mu)^2F_v(t)$ |
|---|---|---|---|---|
| 35.40 | 0 | 0 | 0.0371 | 0.2091 |
| 36.28 | 2 | 0.0010 | 0.0666 | 0.3220 |
| 37.17 | 3.5 | 0.0017 | 0.0974 | 0.4013 |
| 38.05 | 5 | 0.0025 | 0.1494 | 0.5199 |
| 38.94 | 7.5 | 0.0038 | 0.2139 | 0.6214 |
| 39.83 | 10.5 | 0.0053 | 0.3957 | 0.9469 |
| 40.71 | 19 | 0.0097 | 0.5533 | 1.0739 |
| 41.60 | 26 | 0.0133 | 0.7824 | 1.2084 |
| 42.48 | 36 | 0.0184 | 0.9984 | 1.1984 |
| 43.37 | 45 | 0.0230 | 1.370 | 1.2402 |
| 44.25 | 60.5 | 0.0309 | 1.9744 | 1.2968 |
| 45.14 | 85.5 | 0.0437 | 2.2839 | 1.0318 |
| 46.02 | 97 | 0.0496 | 2.6158 | 0.7531 |
| 46.91 | 109 | 0.0557 | 2.9342 | 0.4778 |
| 47.79 | 120 | 0.0613 | 3.3122 | 0.2469 |
| 48.68 | 133 | 0.0680 | 3.4739 | 0.0729 |
| 49.56 | 137 | 0.0700 | 3.5875 | 0.0013 |
| 50.45 | 139 | 0.0711 | 3.5848 | 0.0393 |
| 51.33 | 136.5 | 0.0698 | 3.5397 | 0.1813 |
| 52.22 | 132.5 | 0.0678 | 3.2468 | 0.3884 |
| 53.10 | 119.5 | 0.0611 | 3.0244 | 0.6497 |
| 53.99 | 109.5 | 0.0560 | 2.7091 | 0.9088 |
| 54.87 | 96.5 | 0.0494 | 2.4105 | 1.1580 |
| 55.76 | 84.5 | 0.0432 | 2.0865 | 1.3530 |
| 56.64 | 72 | 0.0368 | 1.7071 | 1.4314 |
| 57.53 | 58 | 0.0297 | 1.3448 | 1.4117 |
| 58.41 | 45 | 0.0230 | 0.9405 | 1.2047 |
| 59.30 | 31 | 0.0158 | 0.3387 | 0.5187 |

Table G.1 (continued)

| t (sec) | $C_e(t)$ | $F_y(t)$ | $tF_y(t)$ | $(t-\mu)^2 F_y(t)$ |
|---|---|---|---|---|
| 60.18 | 11 | 0.0056 | 0.3387 | 0.5187 |
| 61.07 | 5 | 0.0026 | 0.1562 | 0.2813 |
| 61.95 | 4 | 0.0020 | 0.1268 | 0.2646 |
| 62.84 | 3 | 0.0015 | 0.0964 | 0.2305 |
| 63.72 | 2.5 | 0.0013 | 0.0815 | 0.2209 |
| 64.61 | 2 | 0.0010 | 0.0661 | 0.2013 |
| 65.49 | 1.5 | 0.0007 | 0.0503 | 0.1706 |
| 66.38 | 1 | 0.0005 | 0.0340 | 0.1276 |
| 67.26 | 1 | 0.0005 | 0.0344 | 0.1424 |
| 68.15 | 1 | 0.0005 | 0.0349 | 0.1579 |
| 69.03 | 0.5 | 0.0003 | 0.0177 | 0.0871 |
| 69.92 | 0.5 | 0.0003 | 0.0179 | 0.0956 |
| 70.8 | 0.5 | 0.0003 | 0.0181 | 0.1046 |
| 71.69 | 0.5 | 0.0003 | 0.0183 | 0.1140 |
| | 1954.5 | | 50.5315 | 23.0652 |

Therefore $\mu_{packed\ bed}$ = 50.53

$\sigma^2_{packed\ bed}$ = 23.07



Table G.1 Data , mean and variance for blank

| t (sec) | $C_e(t)$ | $F_y(t)$ | $tF_y(t)$ | $(t-\mu)^2 F_y(t)$ |
|---|---|---|---|---|
| 1.8 | 16.2 | 0.6183 | 1.1130 | 0.3531 |
| 3.6 | 9 | 0.3435 | 1.2366 | 0.3746 |
| 5.4 | 1 | 0.0382 | 0.2061 | 0.3087 |
| | 26.2 | | 2.5557 | 1.0365 |

Therefore $\mu_{blank}$ = 2.56 and $\sigma^2_{blank}$ = 1.04

APPENDIX H

BASIC PROGRAMMING FOR CALCULATION OF PECLET NUMBER

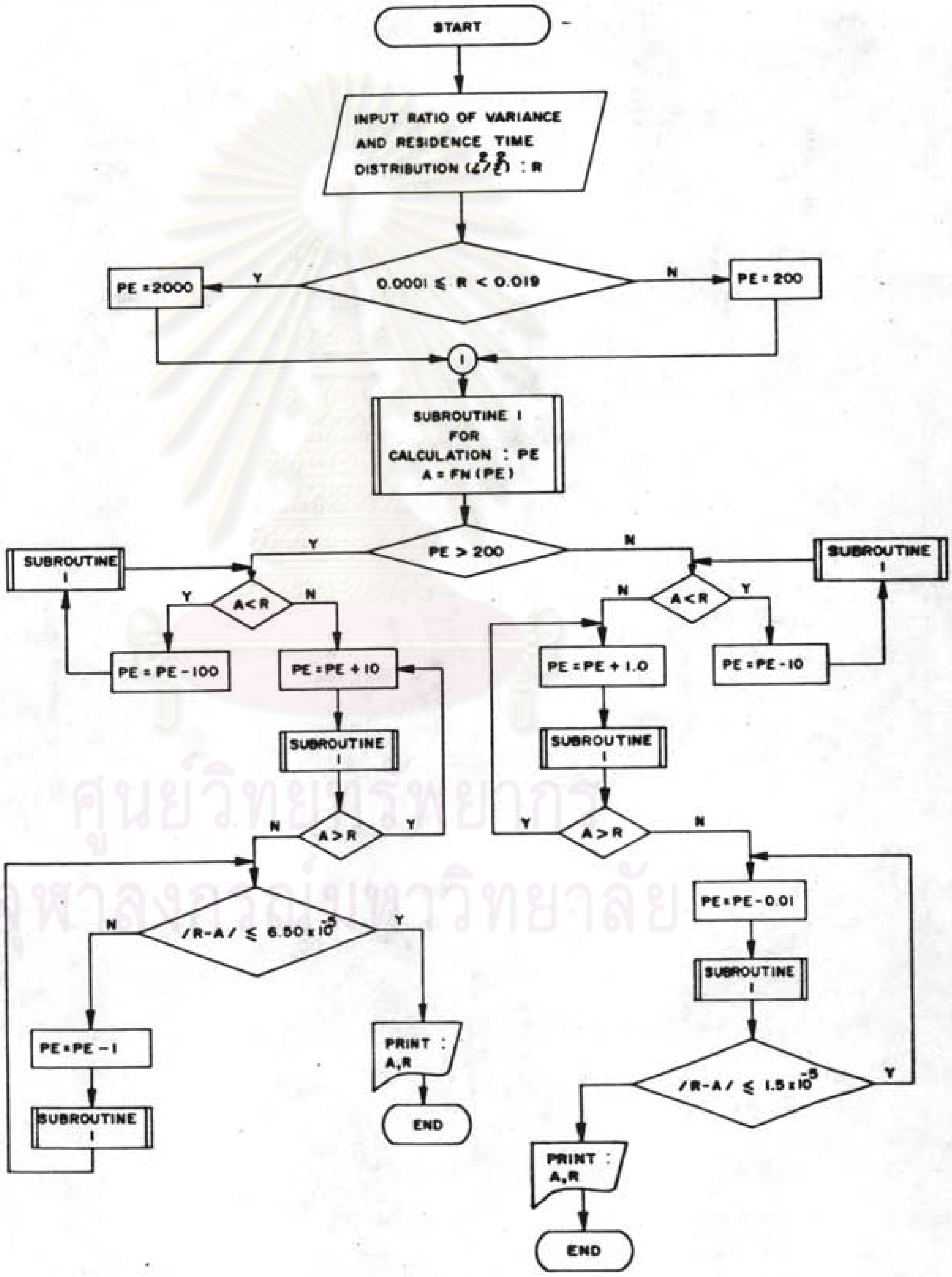

The flow chart shown can be written in basic as follows :

```
5    CLS
10   INPUT " RATIO OF VARIANCE AND SQUARE OF MEAN RESIDENCE TIME "; R
20   IF R >= 0.0001 AND R < 0.019 THEN PE = 2000 : GOTO 40
30   PE = 200
40   GOSUB 250
50   IF PE > 200 THEN 60 ELSE 150
60   IF A < R THEN 70 ELSE 90
70   PE = PE - 100 : GOSUB 250
80   GOTO 60
90   PE = PE + 10
100  GOSUB 250
110  IF A > R THEN 90 ELSE 120
120  IF ABS(R-A) <= 6.5 x 10^-5 THEN 240 ELSE 130
130  Pe = Pe - 1
140  GOSUB 250 : GOTO 120
150  IF A < R THEN 160 ELSE 180
160  Pe = Pe -10
170  GOSUB 250 : GOTO 150
180  Pe = Pe + 1
190  GOSUB 250
200  IF A > R THEN 180 ELSE 210
210  Pe = Pe - 0.1
220  GOSUB 250
230  IF ABS(R-A) <= 1.5 x 10^-5 THEN 240 ELSE 210
240  PRINT A , R : END
250  A = (2/Pe) - (2/Pe^2) + (2/Pe^2)*EXP(-1*Pe)
260  RETURN
```

## APPENDIX I

### EXAMPLES OF CHROMATOGRAPHIC PEAKS

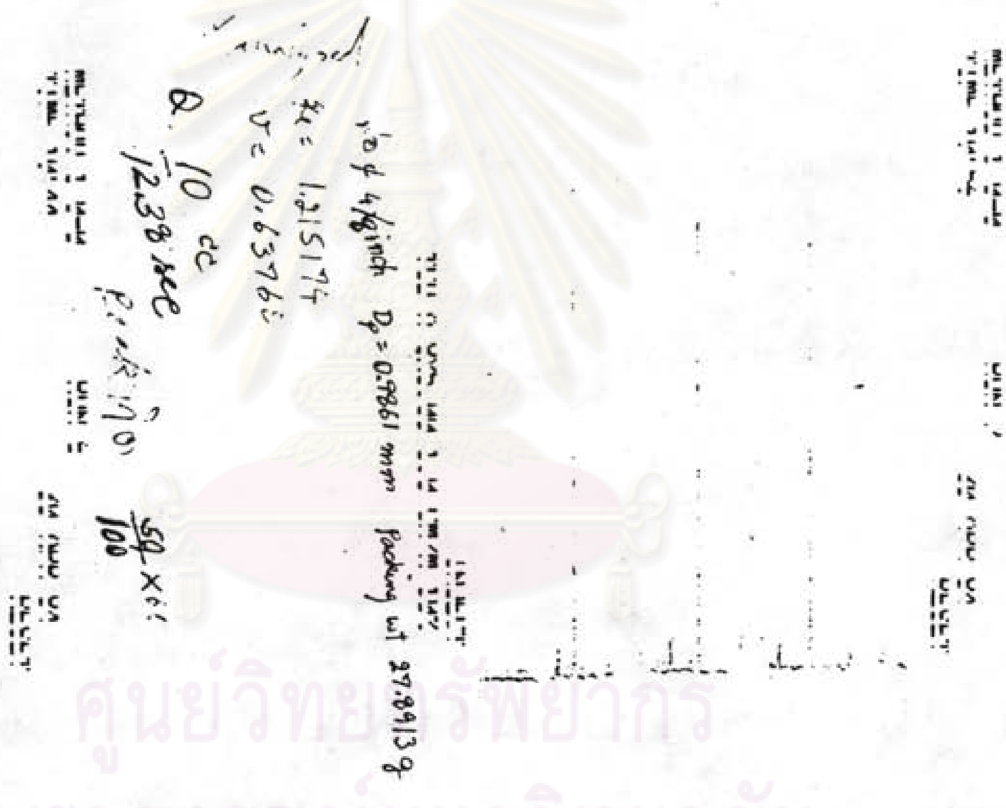



Fig. I1 Three impulse responses of methane tracer in propane at a flow rate of 0.81 cc/sec .

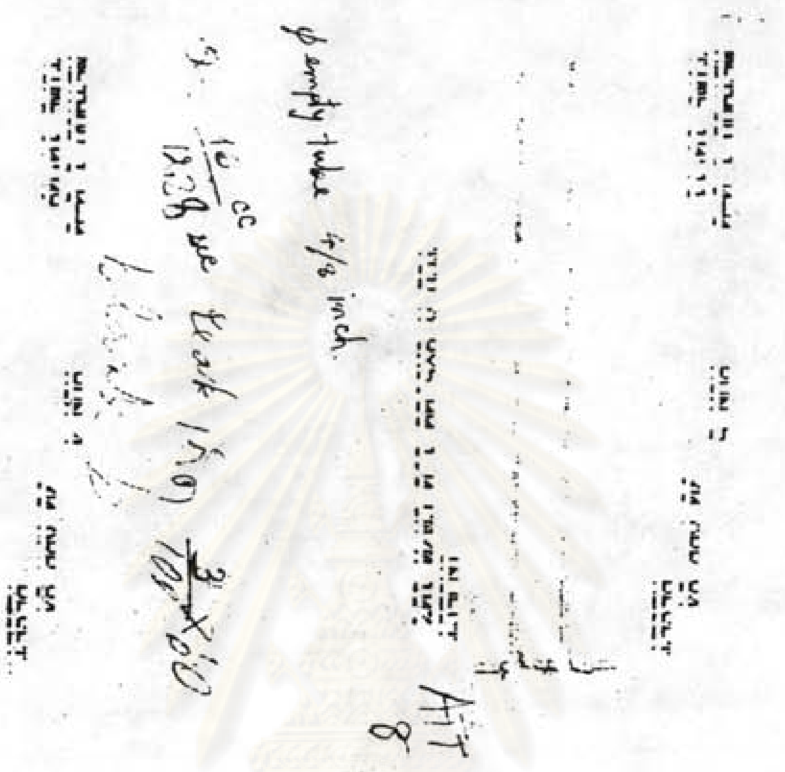


Fig. I2 Two chromatographic peaks of blank performances at flow rate of 0.81 cc/sec .

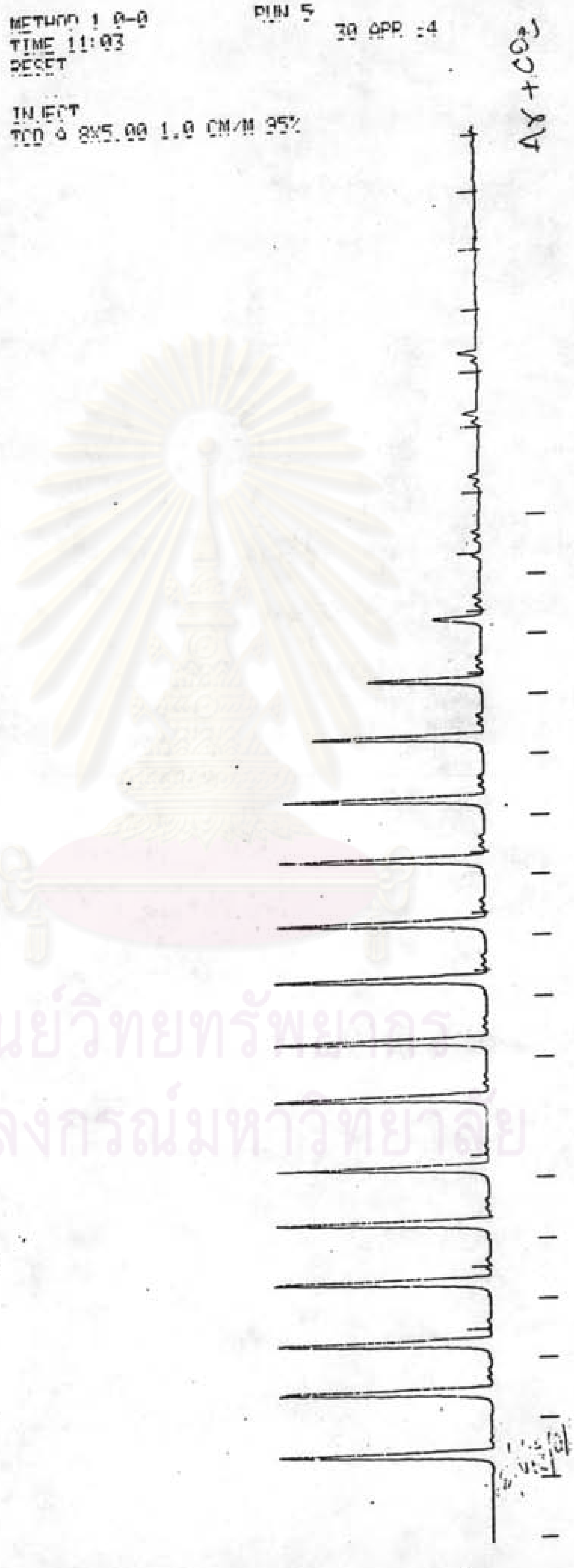


Fig. I3 The chromatogram showing adsorption of carbon dioxide by MSC-3A

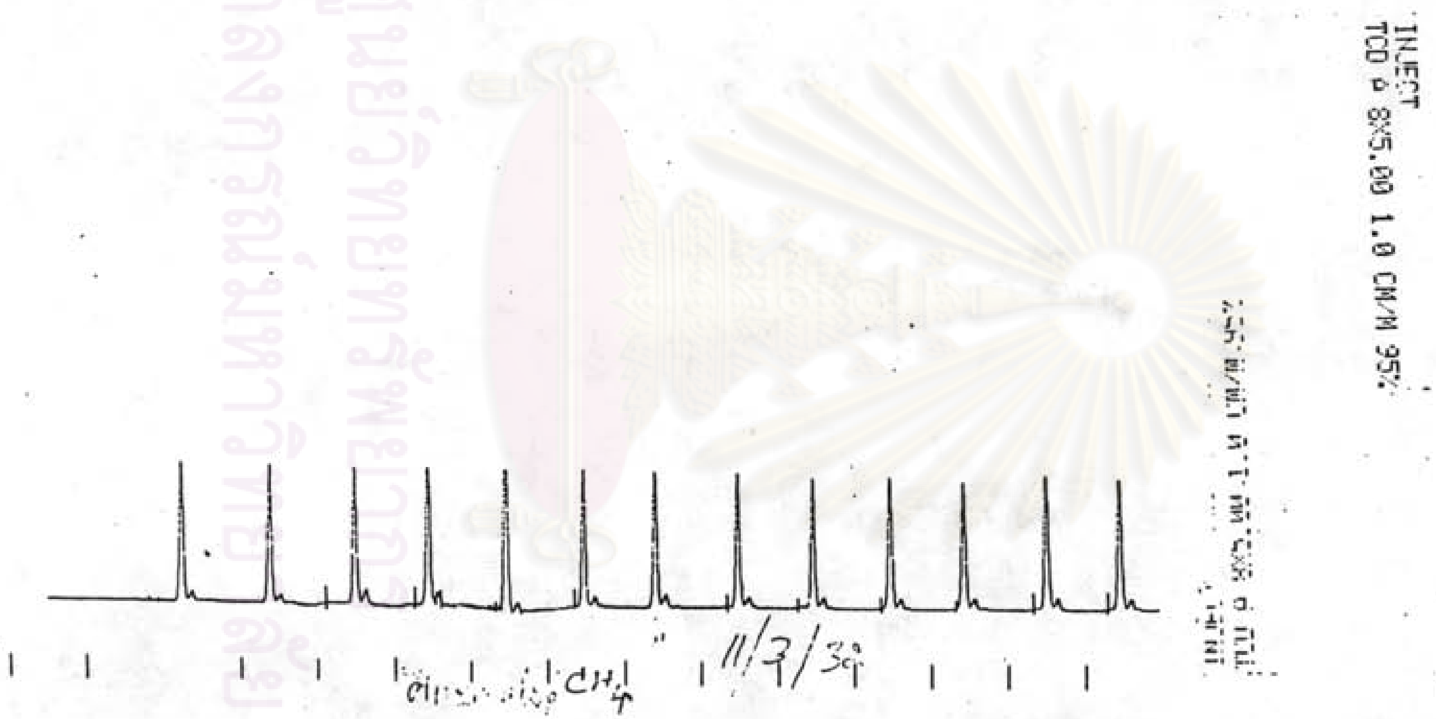


Fig. I4 Chromatograph showing that methane is not adsorbed by MSC-3A adsorbents

# AUTOBIOGRAPHY

Chukiat Chailitilerd received a Bachelor of Pharmay from Chiangmai University in 1985 . He had worked with the Organon (Thailand) Co.,Ltd. He then applied to Chulalongkorn University's Program of Petrochemical Technology in 1987 .